

Status of Spin Physics - Experimental Summary

Jen-Chieh Peng

Physics Division, Los Alamos National Laboratory, Los Alamos, New Mexico, 87545, U.S.A.
and

Department of Physics, University of Illinois, Urbana, Illinois, 61801, U.S.A.

The current status of spin physics experiments, based on talks presented at the Third Circum-Pan-Pacific Symposium on High Energy Spin Physics held in Beijing, 2001, is summarized in this article. Highlights of recent experimental results at SLAC, JLab, and DESY, as well as future plans at these facilities and at RHIC-spin are discussed.

1. Introduction

The purpose of this article is to summarize the experimental status of spin physics based on the material presented at the Third Circum-Pan-Pacific Symposium on High Energy Spin Physics. A total of 12 experimental talks covering recent results and future plans at DESY, JLab, SLAC, and RHIC-spin were presented at this Symposium. These talks successfully convey the sense of excitement in this field through the presentation of many interesting recent experimental results, as well as exciting prospects for future experiments.

Several excellent review articles on high-energy spin physics have been published recently^{1,2,3,4,5}. Many new experimental results were presented at this Symposium for the first time, indicating that spin physics has become one of the most active areas of research in nuclear and particle physics.

The physics topics covered by the 12 experimental talks can be grouped into the following categories:

- Polarized structure functions
 $g_1(x, Q^2)$, $g_2(x, Q^2)$, $h(x, Q^2)$, their integrals, and the GDH sum rule.
- Quark and gluon helicity distributions
 $\Delta q(x, Q^2)$ and $\Delta G(x, Q^2)$.
- Transversity distributions
 $\delta q(x, Q^2)$
- Generalized parton distributions
 Deeply virtual Compton scattering (DVCS).
- Other related topics
 Longitudinal spin transfer in Λ production, exclusive meson productions, A_1^n at large x , etc.

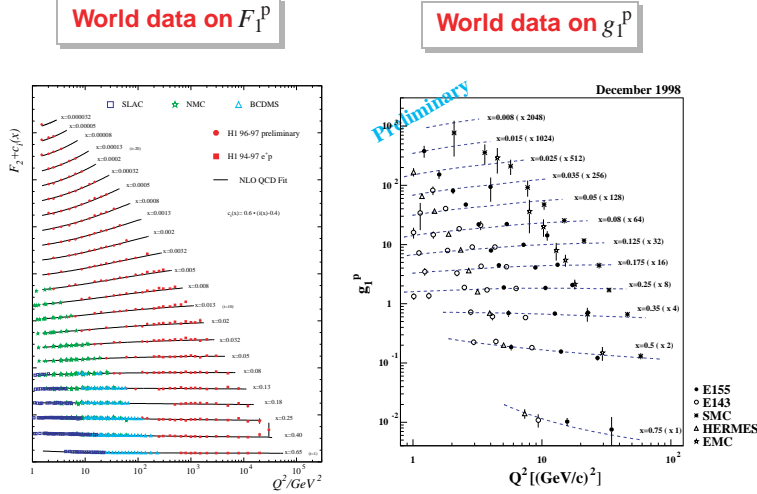


Fig. 1. Collection of $F_1^p(x, Q^2)$ and $g_1^p(x, Q^2)$ data taken from Refs. 3,6.

In the following sections, we will discuss the recent progress in and the future prospects for these various areas of researches.

2. Polarized Structure Functions

2.1. $g_1(x, Q^2)$ and Γ_1

Following the discovery of the “spin-crisis” in the late ’80s, extensive efforts have been devoted to accurate measurements of the spin-dependent structure functions $g_1^p(x, Q^2)$ and $g_1^n(x, Q^2)$. A series of experiments at SLAC (E142, E143, E154, E155, E155x), at CERN (EMC, SMC), and at DESY (HERMES), have measured g_1^p and g_1^n over a broad range of x and Q^2 . Scaling violation of g_1^p is now clearly observed, as shown in Fig. 1. The Q^2 evolution of $g_1^p(x, Q^2)$ is strikingly similar to that of the spin-averaged structure function $F_1^p(x, Q^2)$. In particular, the E155 collaboration recently found⁷ that the ratio $g_1(x, Q^2)/F_1(x, Q^2)$ of all existing data can be parameterized as

$$g_1/F_1 = x^\alpha(a + bx + cx^2)(1 + \beta/Q^2). \quad (1)$$

The values of β , -0.04 ± 0.06 (0.13 ± 0.45) for the proton (neutron), are consistent with zero and indicate that g_1 and F_1 have very similar Q^2 dependences.

The extensive data on $g_1(x, Q^2)$ allow accurate determinations of the integrals $\Gamma_1^{p,n}(Q^2) = \int_0^1 g_1^{p,n}(x, Q^2) dx$ for the proton and the neutron, as well as $\Gamma_1^p(Q^2) - \Gamma_1^n(Q^2)$. Table 1 lists the results of these integrals from recent NLO analysis of existing data by the E155⁷ and SMC^{8,9} collaborations. While the values of Γ_1^p and Γ_1^n are different from the predictions of Ellis and Jaffe¹⁰ who assumed SU(3) flavor symmetry and an unpolarized strange sea, the data are in good agreement with the prediction of the Bjorken sum rule¹¹.

Table 1. Γ_1^p , Γ_1^n , and $\Gamma_1^p - \Gamma_1^n$ from recent NLO analysis.

$Q^2(\text{GeV}^2)$	Γ_1^p	Γ_1^n	$\Gamma_1^p - \Gamma_1^n$	$\Gamma_1^p - \Gamma_1^n$ (theory)	Ref.
5	0.118 ± 0.008	-0.058 ± 0.009	0.176 ± 0.007	0.182 ± 0.005	7
10	0.120 ± 0.016	-0.078 ± 0.021	0.198 ± 0.023	0.186 ± 0.023	8,9
5	0.121 ± 0.018	-0.075 ± 0.021	$0.174 + 0.024 - 0.012$	0.181 ± 0.003	9

As the Bjorken sum rule is now quite well tested, it is not surprising that the experimental activities on $g_1(x)$ are winding down. Nevertheless, there are other interesting aspects of $g_1(x)$ worthy of further studies. First, the behavior of $g_1(x)$ at low x , $x < 0.003$, is not yet known. Perturbative QCD calculations, based on fits to existing data, give predictions for $g_1(x)$ at low x very different from Regge and other models^{12,13}. The largest uncertainty on the Γ_1^p determination also comes from the unmeasured low- x region. Future polarized $e - p$ collider is required for exploring the low- x region¹⁴. Another interesting topics is the behavior of $g_1(x)$ integral at low Q^2 , to be discussed next.

2.2. $\Gamma_1(Q^2)$ at low Q^2 and the generalized GDH integral

How does $\Gamma_1(Q^2)$ evolve as $Q^2 \rightarrow 0$? This question is closely related to the Gerasimov-Drell-Hearn (GDH) sum rule^{15,16}:

$$\int_{\nu_0}^{\infty} [\sigma_{1/2}(\nu) - \sigma_{3/2}(\nu)] \frac{d\nu}{\nu} = -\frac{2\pi^2\alpha}{M^2} \kappa^2. \quad (2)$$

The GDH sum rule, based on general physics principles (causality, unitarity, Lorentz and gauge invariances) and dispersion relation, relates the total absorption cross sections of circularly polarized photons on longitudinally polarized nucleons to the static properties of the nucleons. In Eq. 2, $\sigma_{1/2}$ and $\sigma_{3/2}$ are the photo-nucleon absorption cross sections of total helicity of 1/2 and 3/2, ν is the photon energy and ν_0 is the pion production threshold, M is the nucleon mass and κ is the nucleon anomalous magnetic moment. The GDH sum rule predictions are $-205 \mu\text{b}$ and $-233 \mu\text{b}$ for the proton ($\kappa_p = +1.793$) and neutron ($\kappa_n = -1.913$), respectively.

A first measurement¹⁷ of the helicity dependence of photoabsorption cross section on the proton was recently carried out at MAMI (Mainz) and the contribution to the GDH sum was found¹⁷ to be $-226 \pm 5 \pm 12 \mu\text{b}$ for the photon energy range $200 < \nu < 800 \text{ MeV}$. Using the Unitary Isobar model¹⁸ and a Regge model¹⁹ to estimate the contributions from unmeasured energy regions, the integral is found¹⁷ to be $-210 \mu\text{b}$, consistent with the GDH sum rule. Measurements at higher energies are either underway or being prepared at ELSA, JLab, and SLAC.

The GDH integral in Eq. 2 can be generalized from real photon absorption to virtual photon absorption with non-zero Q^2 :

$$I_{GDH}(Q^2) \equiv \int_{\nu_0}^{\infty} [\sigma_{1/2}(\nu, Q^2) - \sigma_{3/2}(\nu, Q^2)] \frac{d\nu}{\nu}$$

$$= \frac{8\pi^2\alpha}{M} \int_0^{x_0} \frac{g_1(x, Q^2) - \gamma^2 g_2(x, Q^2)}{K} \frac{dx}{x}, \quad (3)$$

where $K = \nu\sqrt{1+\gamma^2}$ is the flux factor of the virtual photon, $\gamma^2 = Q^2/\nu^2$ and $x_0 = Q^2/2M\nu_0$. The generalized GDH integral connects the helicity structures of the nucleons measured in high-energy electron DIS to those in low-energy photo-absorption at the resonance region. Assuming the validity of the Burkhardt - Cottingham sum rule²⁰, $\int_0^1 g_2(x, Q^2)dx = 0$, it follows that for $\gamma \rightarrow 0$ Eq. 3 becomes

$$I_{GDH}(Q^2) = \frac{16\pi^2\alpha}{Q^2} \Gamma_1(Q^2). \quad (4)$$

Eq. 4 shows that the Q^2 -dependence of the generalized GDH integral is directly related to the Q^2 -dependence of Γ_1 . Γ_1^p is known to be positive at high Q^2 and the GDH sum rule (Eq. 2) predicts $\Gamma_1^p = 0$ at $Q^2 = 0$ with a negative slope for $d\Gamma_1^p(Q^2)/dQ^2$, therefore, $\Gamma_1^p(Q^2)$ must become negative at low Q^2 .

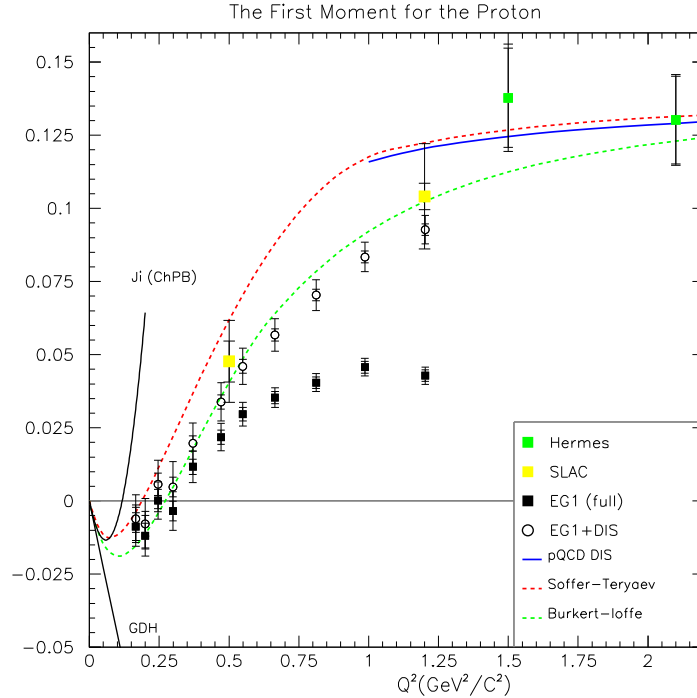


Fig. 2. Preliminary result of $\Gamma_1^p(Q^2)$ from CLAS²¹. Data from SLAC and HERMES are also shown. Theoretical curves are from Refs. 22,23.

The GDH integrals at low Q^2 have recently been measured in several JLab experiments. As reported by Griffioen²¹ in this Symposium, inclusive double spin

asymmetry have been measured at Hall-B using the CLAS spectrometer with polarized electron beams of 2.5 and 4.2 GeV scattered off longitudinally polarized $N\vec{H}_3$ and $N\vec{D}_3$ targets. The kinematical region covered in this experiment corresponds to $0.1 < Q^2 < 2.7 \text{ GeV}^2$ and $W < 2.5 \text{ GeV}$. Preliminary results on $\Gamma_1^p(Q^2)$ extracted from this experiment are shown in Fig. 2. These data indeed show that Γ_1^p changes sign around $Q^2 = 0.3 \text{ GeV}^2$. The origin of the sign-change can be attributed to the competition between $\Delta(1232)$ and higher nucleon resonances. At the lowest Q^2 , the $\Delta(1232)$ has a dominant negative contribution to Γ_1^p . However, at larger Q^2 , higher mass nucleon resonances take over to have a net positive Γ_1^p . As shown in Fig. 2, the strong Q^2 dependence of $\Gamma_1^p(Q^2)$ is well reproduced by the calculation of Burkert and Ioffe²³.

As reported by Chen²⁴ in this Symposium, an extensive spin physics program has been underway using the JLab Hall-A spectrometers. In particular, neutron spin-dependent structure functions, $g_1^n(x, Q^2)$ and $g_2^n(x, Q^2)$, have been measured using an intense polarized electron beam on either longitudinally or transversely polarized ^3He target. Preliminary results²⁴ on the generalized GDH integral for neutron and ^3He are shown in Fig. 3. In contrast to the proton case, the strong negative contribution to the GDH integral from the $\Delta(1232)$ resonance now dominates the entire measured Q^2 range. The data appear to approach the GDH sum rule value at $Q^2 = 0$. However, the data are also consistent with the prediction of Drechsel et al.²⁵ for a rapid variation at very small Q^2 and a departure from the GDH sum rule. Future experiment²⁴ at Hall-A will extend the ^3He measurement down to $Q^2 = 0.02 \text{ GeV}^2$ in order to map out the low Q^2 behavior of the neutron generalized GDH integral.

2.3. Quark-hadron duality

The recent studies at JLab of the spin-averaged and spin-dependent structure functions at low Q^2 region have shed new light on the subject of quark-hadron duality. Thirty years ago, Bloom and Gilman²⁶ noticed that the structure functions obtained from deep-inelastic scattering experiments, where the substructures of the nucleon are probed, are very similar to the averaged structure functions measured at lower energy, where effects of nucleon resonances dominate. This surprising similarity between the resonance electroproduction and the deep inelastic scattering suggests a common origin for these two phenomena, called local duality.

Recently, high precision data²⁷ from JLab have verified the quark-hadron duality for spin-averaged scattering on proton and deuteron targets. For Q^2 as low as 0.5 GeV^2 , the resonance data are within 10% of the DIS results. When the mean F_2 curve from the resonance data is plotted as a function of the Nachtmann variable, $\xi = 2x/(1 + \sqrt{1 + 4M^2x^2/Q^2})$, it resembles the xF_3 structure function obtained in neutrino scattering experiments. Since xF_3 is a measure of the valence quark distributions, the similarity between xF_3 and the mean F_2 suggests that the F_2 structure function at low Q^2 originates from valence quarks only.

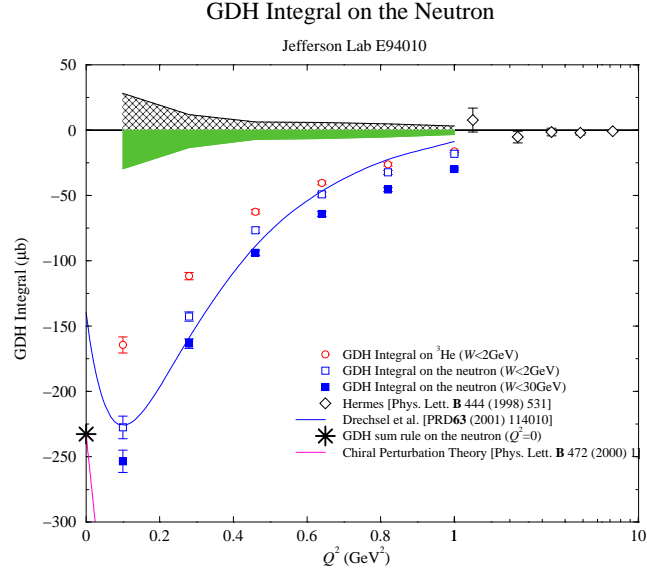


Fig. 3. Near final results of the JLab Hall-A measurement²⁴ of the Generalized GDH sum for neutron and ^3He .

It is of much interest to extend the study of quark-hadron duality to spin-dependent structure functions. In this Symposium, Griffioen²¹ presented the preliminary result from CLAS showing that quark-hadron duality is also observed in g_1^p . A comparison of $g_1^p(\xi)$ between the resonance data and the Gehrman and Stirling²⁸ parameterization of the DIS data shows a good agreement for $\xi > 0.2$ (the valence quark region). At $\xi < 0.2$, the resonance data appear to deviate from the DIS data. This trend is reminiscent of what was observed for the spin-averaged structure functions²⁷. Additional information on the quark-hadron duality is also expected from the JLab Hall-A measurement²⁴ of $g_1^n(\xi)$ for neutrons.

2.4. $g_2(x, Q^2)$

Unlike the spin structure function g_1 , which has a clear interpretation in the quark-parton model (QPM), the g_2 structure function is sensitive to higher-twist quark-gluon correlation effect and is not readily interpreted in QPM. The g_2 structure function probes both the transverse and the longitudinal parton distributions in the nucleons. Using the operator product expansion (OPE) technique^{29,30} in QCD, g_2 can be expressed in terms of three components³¹: a leading twist-2 part $g_2^{WW}(x, Q^2)$ originating from the same set of operators that contribute to g_1 , another twist-2 structure function $h_T(x, Q^2)$ depicting quark transverse polarization, and a twist-3 part from quark-gluon interactions $\xi(x, Q^2)$,

$$g_2(x, Q^2) = g_2^{WW}(x, Q^2) - \int_x^1 \frac{\partial}{\partial y} \left(\frac{m}{M} h_T(y, Q^2) + \xi(y, Q^2) \right) \frac{dy}{y}, \quad (5)$$

where m and M are quark and nucleon masses. The twist-2 contribution, g_2^{WW} , is related to g_1 via³²

$$g_2^{WW}(x, Q^2) = -g_1(x, Q^2) + \int_x^1 \frac{g_1(y, Q^2)}{y} dy. \quad (6)$$

The contribution from the transversity distribution $h_T(x, Q^2)$ is suppressed by the m/M term and can be neglected. Hence, the difference between g_2 and g_2^{WW} , $\overline{g_2} = g_2 - g_2^{WW}$, will isolate the twist-3 contribution.

The moments of g_1 and g_2 can be derived from OPE:

$$\begin{aligned} \int_0^1 x^n g_1(x, Q^2) dx &= \frac{a_n}{2}, & n = 0, 2, 4, \dots \\ \int_0^1 x^n g_2(x, Q^2) dx &= \frac{1}{2} \frac{n}{n+1} (d_n - a_n), & n = 2, 4, 6, \dots, \end{aligned} \quad (7)$$

where a_n and d_n are the twist-2 and twist-3 matrix elements of the renormalized operators, respectively. The twist-3 matrix elements d_n can then be evaluated using

$$d_n = \frac{2(n+1)}{n} \int_0^1 x^n \overline{g_2}(x, Q^2) dx. \quad (8)$$

A primary goal for measuring g_2 is therefore to determine the twist-3 contribution which reflects quark-gluon correlation effects. A series of SLAC experiments, E142, E143, E154, E155 and E155x, have measured $g_2(x, Q^2)$ for protons and neutrons. In this Symposium, Bosted³³ reported the near-final results of g_2^p and g_2^d from E155x. The x -dependence of all SLAC g_2^p data is reasonably well described by the twist-2 component g_2^{WW} . However, the data also allow non-zero twist-3 contributions. In particular, the twist-3 matrix elements, d_2^p and d_2^n , evaluated using Eq. 8, are shown to be small but non-zero³³. Meizani³⁴ discussed in this Symposium a proposal to measure g_2^n with high accuracy at the proposed 12 GeV CEBAF upgrade using a polarized ^3He target and a large acceptance spectrometer. This could provide a definitive result on the twist-3 content of the nucleon.

The new $g_2(x)$ data from E155x also allow evaluations of the integrals $\int g_2(x) dx$ in order to check the Burkhardt-Cottingham sum rule. In this Symposium, Bosted³³ reported that for $0.02 \leq x \leq 0.8$ at $Q^2 = 5 \text{ GeV}^2$, the integral was found to be -0.034 ± 0.008 for proton and -0.002 ± 0.011 for deuteron. The apparent disagreement between the proton result and the Burkhardt-Cottingham sum rule could be due to the contribution of the unmeasured small x region. Another sum rule by Efremov, Leader and Teryaev (ELT)³⁵, derived with the assumption of isospin symmetry of the sea-quark distributions, gives

$$\int_0^1 x [g_1^p(x) + 2g_2^p(x) - g_1^n(x) - 2g_2^n(x)] dx = 0. \quad (9)$$

The ELT sum rule is much less sensitive to the small- x uncertainty due to the factor x in the integrand. The most recent value of this integral for the proton is found³³

to be -0.009 ± 0.008 at $Q^2 = 2.5 \text{ GeV}^2$, consistent with the prediction of the sum rule. The recent JLab Hall-A data²⁴ on g_2^n could provide a further check of this sum rule for the neutron.

3. Polarized Quark and Gluon Distributions

3.1. Polarized quark and antiquark distributions

The $g_1(x, Q^2)$ data obtained in inclusive DIS have been analyzed⁸ in the framework of NLO QCD to extract information on $\Delta\Sigma(x)$, $\Delta q_{NS}^{p,n}(x)$, and $\Delta g(x)$, where $\Delta\Sigma$ and Δq_{NS} correspond to the flavor-singlet and flavor-nonsinglet quark polarization, and Δg is the gluon polarization. The inclusive DIS data, however, do not allow a detailed flavor decomposition of the nucleon spin. In particular, the contributions from valence and sea quarks are not separated. To overcome this limitation, the SMC and HERMES experiments have advocated the use of semi-inclusive deep inelastic scattering (SIDIS), where the leading hadrons accompanying the DIS process are also detected. The flavor of the struck quark is expected to be reflected by the flavor of the produced hadrons. Hence the hadrons provide a “tag” on the flavor of the struck quark. This technique was first applied by the SMC^{36,37} collaboration to determine Δu_v , Δd_v , and $\Delta\bar{q}$ ($\Delta\bar{u} = \Delta\bar{d} = \Delta\bar{q}$). Later, the HERMES collaboration used this method to measure the $\bar{d} - \bar{u}$ flavor asymmetry of the unpolarized nucleon sea and obtained³⁸ a result consistent with that from a completely different approach^{39,40,41} using the Drell-Yan process. This agreement suggests that the SIDIS is indeed a valid tool for studying flavor decomposition.

Extensive SIDIS data have been collected⁴² by the HERMES collaboration on polarized gas targets of H , D , and ^3He . Shibata⁴³ and Bernreuther⁴⁴ presented in this Symposium the preliminary results of Δu_v , Δd_v , and $\Delta\bar{u}$ based on an analysis of the HERMES data collected up to Spring '99. As shown in Fig 4, the HERMES data have improved accuracy over the SMC data. Both the SMC and the HERMES results are in very good agreement with the parameterization of Gehrmann and Stirling²⁸. In order to increase the statistical significance, the constraint

$$\Delta\bar{q}/\bar{q} = \Delta u_s/u_s = \Delta\bar{u}/\bar{u} = \Delta d_s/d_s = \Delta\bar{d}/\bar{d} = \Delta\bar{s}/\bar{s} = \Delta s/s \quad (10)$$

has been imposed in the analysis shown in Fig. 4.

With the large sample of polarized $e^+ + d$ SIDIS data collected during 1999 and 2000 in conjunction with an operational RICH detector for $\pi/K/p$ identification, the HERMES collaboration is now analyzing their SIDIS data without the constraint of Eq. 10. The identification of kaons with the RICH detector would help isolating the Δs component. The anticipated statistical accuracy for Δu_v , Δd_v , $\Delta\bar{u}$, $\Delta\bar{d}$, and $\Delta s (= \Delta\bar{s})$ in this 5-parameter analysis is shown in Fig. 5. The HERMES analysis could lead to exciting first results on the flavor structure of the sea-quark polarizations. Several interesting issues, such as the large flavor asymmetry between the $\Delta\bar{u}$ and $\Delta\bar{d}$ predicted⁴⁵ in the chiral-quark-soliton model as well as the negative

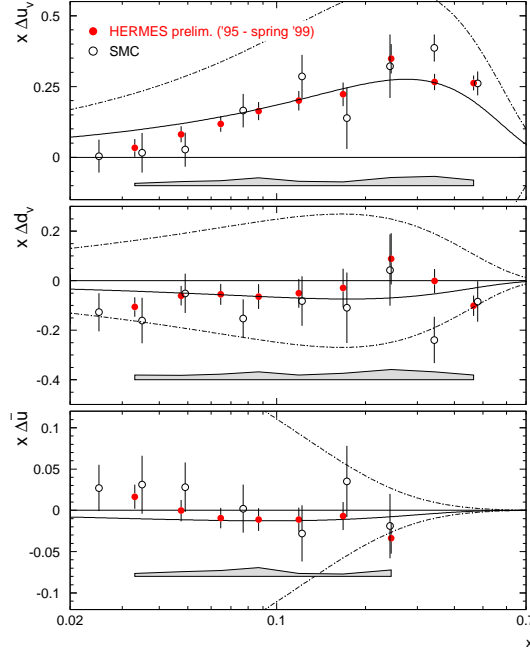


Fig. 4. Preliminary result of the HERMES analysis of SIDIS data⁴⁴. The data are presented at a common Q^2 of 2.5 GeV^2 . The dashed dotted lines indicate the positivity limit and the solid lines show parameterizations from Gehrmann and Stirling.

strange-quark polarization expected from the analysis of g_1 , could be addressed. The result of the five-parameter analysis is expected⁴³ to be available soon.

Another promising technique for measuring sea-quark polarization is W -boson production^{46,47} at RHIC. The longitudinal single-spin asymmetry for W production in $\vec{p} + p \rightarrow W^\pm + x$ can be written in leading order as

$$A_L^{W^+} = \frac{\Delta u(x_1)\bar{d}(x_2) - \Delta\bar{d}(x_1)u(x_2)}{u(x_1)\bar{d}(x_2) + \bar{d}(x_1)u(x_2)}, \quad A_L^{W^-} = \frac{\Delta d(x_1)\bar{u}(x_2) - \Delta\bar{u}(x_1)d(x_2)}{d(x_1)\bar{u}(x_2) + \bar{u}(x_1)d(x_2)}, \quad (11)$$

where $x_{1,2}$ are the Bjorken- x of the colliding quarks and antiquarks. For $x_1 \ll x_2$, Eq. 11 becomes

$$A_L^{W^+} \approx -\frac{\Delta\bar{d}(x_1)}{\bar{d}(x_1)}, \quad A_L^{W^-} \approx -\frac{\Delta\bar{u}(x_1)}{\bar{u}(x_1)}, \quad (12)$$

and A_L gives a direct measure of sea-quark polarization. For $x_1 \gg x_2$, one obtains

$$A_L^{W^+} \approx -\frac{\Delta u(x_1)}{u(x_1)}, \quad A_L^{W^-} \approx -\frac{\Delta d(x_1)}{d(x_1)}, \quad (13)$$

and the valence quark polarization is probed. In this Symposium, Kiryluk⁴⁸ discussed the plan to measure $W^\pm \rightarrow e^\pm + x$ at the STAR collaboration. The PHENIX collaboration is capable of measuring the $W^\pm \rightarrow \mu^\pm + x$ decays as well, as discussed

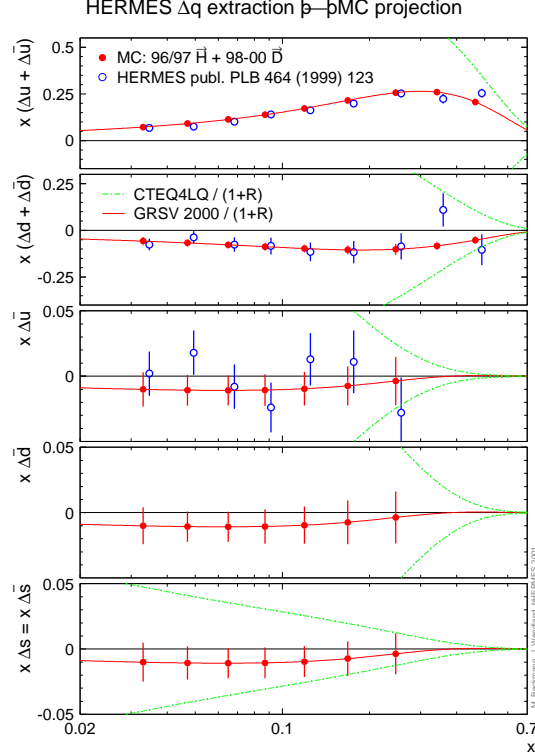


Fig. 5. Monte Carlo prediction for the statistical precision on the extraction of polarized quark distributions times Bjorken x after analyzing all HERMES data taken up to summer 2000⁴⁴. The Monte Carlo points have been placed on the parameterization curve from GRSV2000. The dashed dotted lines represent the positivity limit based on the unpolarized CTEQ4LQ parton distribution functions.

by Saito⁴⁹. The RHIC W -production and the PHENIX SIDIS measurements are clearly complementary tools for determining polarized quark and antiquark distributions.

3.2. Polarized gluon distribution

Analysis of existing g_1 data showed that only $\sim 30\%$ of the nucleon's spin is carried by quarks. This suggests that gluons could have a large polarization. A NLO analysis of $g_1(x, Q^2)$ by the SMC collaboration⁸ showed that $\Delta G(x)$ is positive, albeit with a large uncertainty. Global fits²⁸ to existing spin-dependent structure functions can also accommodate very different parameterizations of $\Delta G(x)$, again showing that gluon polarization is poorly known. A direct and precise determination of $\Delta G(x)$ remains one of the most important goals of spin physics.

Although inclusive DIS does not directly probe the gluon distribution, certain semi-inclusive DIS processes are sensitive to ΔG . The HERMES collaboration has

reported a measurement⁵⁰ of $\Delta G/G$ at $x \approx 0.17$ using semi-inclusive hadron-pair production. Lepto- and photo- open-charm production has also been proposed at CERN⁵¹ and at SLAC^{33,52} for $\Delta G/G$ measurements.

Polarized proton-proton collision at RHIC offers a great opportunity for studying gluon polarization. In this Symposium, Kiryluk⁴⁸ discussed the proposed double longitudinal spin asymmetry, A_{LL} , measurement for $\vec{p} + \vec{p} \rightarrow \gamma + jet + x$ at STAR and Liu⁵³ discussed the heavy-quark production at PHENIX. Other processes sensitive to ΔG are the inclusive prompt photon production, jet production, and high- p_T hadron production. Although no new experimental results on $\Delta G(x)$ were presented in this Symposium, it is clear that a wealth of new results will be forthcoming.

4. Transversity Distributions

In addition to the unpolarized and polarized quark distributions, $q(x, Q^2)$ and $\Delta q(x, Q^2)$, a third quark distribution, called transversity, is the remaining twist-2 distribution yet to be measured. This helicity-flip quark distribution, $\delta q(x, Q^2)$, can be described in QPM as the net transverse polarization of quarks in a transversely polarized nucleon. The corresponding structure function is given by

$$h_1(x, Q^2) = \frac{1}{2} \sum_i e_i^2 \delta q_i(x, Q^2). \quad (14)$$

Due to the chiral-odd nature of the transversity distribution, it can not be measured in inclusive DIS experiments. In order to measure $\Delta q(x, Q^2)$, an additional chiral-odd object is required. For example, the double spin asymmetry, A_{TT} , for Drell-Yan cross section in transversely polarized pp collision, is sensitive to transversity since $A_{TT} \sim \sum_i e_i^2 \delta q_i(x_1) \delta \bar{q}_i(x_2)$. Such a measurement could be carried out at RHIC^{2,49}, although the anticipated effect is small, on the order of 1 – 2%.

Several other methods for measuring transversity have been proposed for semi-inclusive DIS. In particular, Collins suggested⁵⁴ that a chiral-odd fragmentation function in conjunction with the chiral-odd transversity distribution would lead to an observable single-spin azimuthal asymmetry in semi-inclusive pion production. An analysis of the jet structure in $Z^0 \rightarrow 2$ jets decay suggested that the Collins function has a sizable magnitude⁵⁵.

As reported by Schnell⁵⁶ in this Symposium, the HERMES collaboration has recently measured⁵⁸ single-spin azimuthal asymmetry for charged and neutral pion electroproduction. Using unpolarized positron beam on a longitudinally polarized hydrogen target, the cross section was found to have a $\sin\phi$ dependence, where ϕ is the azimuthal angle between the pion and the (e, e') scattering plane. This Single-Spin-Asymmetries (SSA) can be expressed as the analyzing power in the $\sin\phi$ moment, and the result is shown in Fig. 6 for π^+ , π^- , and π^0 as a function of the pion fractional energy z , the Bjorken x , and the pion transverse momentum P_\perp . The $\sin\phi$ moment for an unpolarized (U) positron scattered off a longitudinally (L) polarized target contains two main contributions

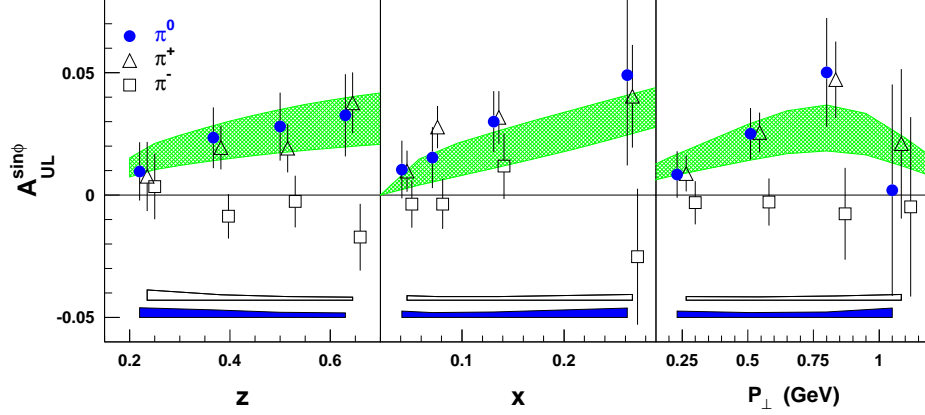


Fig. 6. Analyzing power in the $\sin\phi$ moment from HERMES^{57,58}. Error bars include the statistical uncertainty only. The filled and open bands at the bottom of the panels represent the systematic uncertainties for neutral and charged pions, respectively. The shaded areas show a range of predictions of a model calculation applied to the case of π^0 electro-production^{59,60}.

$$\begin{aligned} \langle \sin\phi \rangle \propto S_L \frac{2(2-y)}{Q\sqrt{1-y}} \sum_q e_q^2 x h_L^q(x) H_1^{\perp,q}(z) \\ + S_T(1-y) \sum_q e_q^2 x h_1^q(x) H_1^{\perp,q}(z), \end{aligned} \quad (15)$$

where S_L and S_T are the longitudinal and transverse components of the target spin orientation with respect to the virtual photon direction. For the HERMES experiment with a longitudinally polarized target, the transverse component is nonzero with a mean value of $S_T \approx 0.15$. The observed azimuthal asymmetry could be a combined effect of the h_1 transversity and the twist-3 h_L distribution. Figure 6 shows that a model calculation^{59,60} reproduces the z , x , and P_\perp dependences of the π^0 asymmetry quite well. The striking difference between the π^+ and π^- analyzing power suggests that the Collins fragmentation function is sizable only when the flavor of the struck quark is present in the final hadron.

If the azimuthal asymmetry observed by HERMES is indeed caused by the h_1 transversity, a much larger asymmetry is expected for a transversely polarized target. An earlier SMC measurement had limited statistics and was inconclusive⁶¹. The HERMES Collaboration plans to measure⁵⁶ the shape of $\delta u(x)$ (and $H_1^{\perp,u}(z)$) using a transversely polarized proton target in 2002-03. A proposal to measure $\delta d(x)$ using a transversely polarized deuterium target has also been discussed⁶².

5. Generalized Parton Distributions and DVCS

There has been intense theoretical and experimental activities in recent years on the subject of Generalized Parton Distribution (GPD). In the Bjorken scaling regime,

exclusive leptonproduction reactions can be factorized into a hard-scattering part calculable in QCD, and a non-perturbative part parameterized by the GPDs. The GPD takes into account dynamical correlations between partons with different momenta. In addition to the dependence on Q^2 and x , the GPD also depends on two more parameters, the skewedness ξ and the momentum transfer to the baryon, t . Of particular interest is the connection between GPD and the nucleon's orbital angular momentum⁶³.

The deeply virtual Compton scattering (DVCS), in which an energetic photon is produced in the reaction $ep \rightarrow ep\gamma$, is most suitable for studying GPD. Unlike the exclusive meson productions, DVCS avoids the complication associated with mesons in the final state and can be cleanly interpreted in terms of GPDs. An important experimental challenge, however, is to separate the relatively rare DVCS events from the abundant electromagnetic Bethe-Heitler (BH) background. Significant progress has been made recently, and several experiments at HERA and JLab have reported observation of the DVCS events. From the collision of 800 GeV protons with 27.5 GeV positrons, both the ZEUS⁶⁴ and the H1⁶⁵ collaborations at DESY observed an excess of $e^+ + p \rightarrow e^+ + \gamma + p$ events in a kinematic region where the BH cross section is largely suppressed. The excess events were attributed to the DVCS process and the H1 collaboration further determined⁶⁵ the DVCS cross section over the kinematic range $2 < Q^2 < 20 \text{ GeV}^2$, $30 < W < 120 \text{ GeV}$, and $|t| < 1 \text{ GeV}^2$. (The x range covered is roughly $0.00035 < x < 0.0035$ for $W = 75 \text{ GeV}$.)

At lower c.m. energies, the HERMES⁶⁶ and the CLAS⁶⁷ collaborations observed the interference between the DVCS and the BH processes, which manifests itself as a pronounced azimuthal asymmetry correlated with the beam helicity. In this Symposium, Bianchi⁶⁸ reported the HERMES measurement⁶⁶ shown in Fig. 7. The HERMES result is in nice agreement with the CLAS result⁶⁷, also shown in Fig. 7. Note that there exists several differences between these two measurements. First, the beam energy for the CLAS experiment (4.25 GeV) is lower than for the HERMES experiment (27.6 GeV). Second, the CLAS experiment detected the electron and proton, while the HERMES experiment measured the positron and the photon in the final state. Finally, a polarized electron beam was used for CLAS instead of the polarized positron beam for HERMES. The qualitative agreement between these two experiments is reassuring. It is interesting to note that the CLAS data showed an opposite sign for the azimuthal asymmetry relative to the HERMES data (in Fig. 7 the offsets of the azimuthal ϕ angle are different for the two experiments). This is to be expected since the interference term is proportional to the sign of the lepton charge.

As discussed by Bianchi⁶⁸ in this Symposium, another observable sensitive to the interference between the DVCS and the BH processes is the azimuthal asymmetry between unpolarized e^+ and e^- beams. In contrast to the Beam Spin Asymmetry (BSA) which is sensitive to the imaginary part of the DVCS amplitudes, the Beam Charge Asymmetry (BCA) is probing the real part of the DVCS amplitudes⁶⁹. Analysis of the HERMES e^- data in 98-99 and the e^+ data in 99-00 is underway,

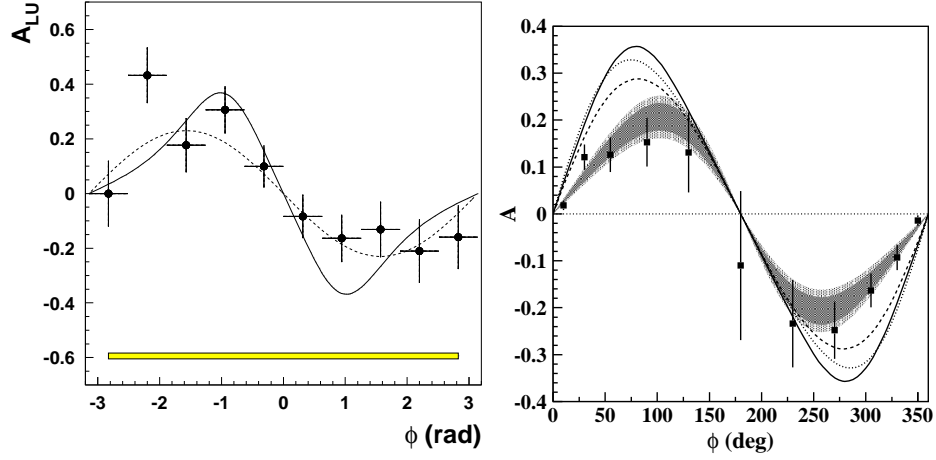


Fig. 7. Left panel: HERMES data⁶⁶ on the beam-spin asymmetry for hard exclusive electroproduction of photons as a function of the azimuthal angle ϕ . Right panel: CLAS data⁶⁷ on the beam-spin asymmetry resulting from the DVCS-BH interference.

and the first result on the BCA is expected soon⁶⁸.

6. Other Related Topics

6.1. Λ polarization

Schnell⁵⁶ described the recent progress at HERMES on semi-inclusive Λ production. The HERMES collaboration has measured the longitudinal spin transfer from the polarized electron beam to the Λ particle in the final state, as well as the transverse Λ polarization using unpolarized beam. The main interest for the longitudinal spin transfer measurement is to deduce information on the polarized quark distribution in the Λ . Assuming u -quark dominance as well as helicity conservation in the $u \rightarrow \Lambda$ fragmentation process, the HERMES measurement of the longitudinal spin transfer can reveal the role of u quark for Λ spin. Earlier measurements^{70,71} of Λ polarization from Z decays are sensitive to s quark polarization in the Λ . The NOMAD collaboration has also measured^{72,73} Λ and $\bar{\Lambda}$ polarization in neutrino DIS.

The new HERMES measurement⁵⁶ covers a kinematic range (roughly $0.2 < z < 0.8$ and $0 < x_F < 0.8$) much broader than previous DIS experiments^{74,75}. Preliminary result on the average spin transfer in this kinematic region is 0.04 ± 0.09 . The x_F dependence is consistent with the previous NOMAD result⁷². The predictions of several model calculations^{76,77} for a rising spin transfer with increasing z are not observed in the data, although the statistical accuracy is limited. A new detector was installed at HERMES to enhance the acceptance of Λ detection for future measurements⁵⁶.

6.2. Exclusive electroproduction of mesons

New results on exclusive meson production from HERMES and CLAS collaborations have been presented in this Symposium. The current interest in hard exclusive processes is largely due to the fact that QCD factorization was proved to be valid for exclusive meson production with longitudinal virtual photons⁷⁸. Such factorization allowed new means to extract the unpolarized and polarized GPD. In particular, unpolarized GPDs can be measured with exclusive vector meson production, while polarized GPDs can be probed via exclusive pseudoscalar meson production.

Bianchi⁶⁸ presented the preliminary HERMES results on the longitudinal component of the exclusive ρ and ϕ meson production cross sections. The data are in good agreement with a calculation⁷⁹ based on GPD. For exclusive pseudoscalar meson production, the HERMES collaboration measured the single spin azimuthal asymmetry in the reaction $e^+ + \vec{p} \rightarrow e'^+ + n + \pi^+$. The asymmetry is found^{68,80} to be very large ($-0.18 \pm 0.05 \pm 0.02$) and has a sign opposite to that of inclusive π^+ production⁵⁷.

The CLAS collaboration recently reported^{21,81} the first measurement of double spin asymmetry in the $\vec{e} + \vec{p} \rightarrow e' + \pi^+ + n$ reaction. This observable is sensitive to the contributions from various resonances, and the data indicate the dominance of the helicity-1/2 contribution in the second and third resonance regions.

6.3. A_1^n at large x

A new measurement²⁴ of the A_1^n spin asymmetry has been carried out at Hall-A in JLab using polarized ^3He target. The value of A_1^n as $x \rightarrow 1$ is sensitive to the underlying models describing valence quark dynamics in the nucleon. Isospin and SU(6) symmetries predict $A_1^n \rightarrow 1$ as $x \rightarrow 1$, while pQCD approaches^{82,83} predict $A_1^n \rightarrow 0$ as x approaches 1. Preliminary JLab result²⁴ for A_1^n in the $0.33 < x < 0.61$ range show that A_1^n turns positive for large x . A definitive measurement of A_1^n with high accuracy at very large x has been considered for the 12 GeV CEBAF upgrade³⁴.

7. Summary and Outlook

There has been an enormous progress in various areas of spin physics experiments since the last Circum-Pan-Pacific Spin Symposium in 1999. An incomplete list of the major progress would include the following:

- First JLab measurements on spin structure functions have provided new information on $g_1^p, g_1^n, g_2^n, \Gamma_1^p, \Gamma_1^n$ and the generalized GDH sum at the resonance region.
- Observation of the azimuthal Single Spin Asymmetry at HERMES in semi-inclusive pion production holds a great promise for measuring transversity in the near future.

- Observation of the DVCS process at HERMES and JLab has generated much interest and could develop into an extensive program for measuring Generalized Parton Distributions.
- Various spin observables in exclusive meson electroproductions are being measured at HERMES and JLab.
- Commissioning of the RHIC-spin has been successfully carried out⁸⁴.

Many new results are anticipated in the near future:

- First results from RHIC-spin.
- First results on $\Delta\bar{u}$, $\Delta\bar{d}$ and $\Delta s(= \Delta\bar{s})$ from the 5-parameter analysis of the HERMES SIDIS data.
- First measurement of the transversity (δu) at HERMES using transversely polarized targets.
- Precise data on DVCS from HERMES and JLab.
- $\Delta G(x)$ from SLAC, COMPASS, HERMES, and RHIC-spin.
- Additional low- Q^2 data from JLab.
- And much more

Acknowledgements

I would like to thank Professor Bo-Qiang Ma for inviting me to attend this very interesting and successful symposium.

References

1. B. W. Filippone and X. Ji, hep-ph/0101224.
2. G. Bunce, N. Saito, J. Soffer, and W. Vogelsang, *Ann. Rev. Nucl. Part. Sci.* **50**, 525 (2000).
3. R. L. Jaffe, hep-ph/0101224.
4. M. Anselmino, hep-ph/0107093.
5. N. Bianchi and R. Jakob, hep-ph/0108078.
6. N. C. R. Makins, Talk presented at DIS2000.
7. The E155 Collaboration, P. L. Anthony *et al.*, *Phys. Lett.* **B493**, 19 (2000).
8. The SMC Collaboration, B. Adeva *et al.*, *Phys. Rev.* **D58**, 112001 (1998).
9. The SMC Collaboration, B. Adeva *et al.*, *Phys. Rev.* **D58**, 112002 (1998).
10. J. Ellis and R. Jaffe, *Phys. Rev.* **D9**, 1444 (1974); **D10**, 1669 (1974).
11. J. D. Bjorken, *Phys. Rev.* **148**, 1467 (1966); **D1**, 1376 (1970).
12. F. E. Close and R. G. Roberts, *Phys. Lett.* **B336**, 257 (1994).
13. J. Kwiecinski and B. Ziaja *Phys. Rev.* **D60**, 054004 (1999).
14. V. W. Hughes and A. Deshpande, *Nucl. Phys. Proc. Suppl.* **79**, 579 (1999), hep-ex/9906006.
15. S. B. Gerasimov, *Sov. J. Nucl. Phys.* **2**, 430 (1966).
16. S. D. Drell and A. C. Hearn, *Phys. Rev. Lett.* **16**, 430 (1966).
17. The GDH and A2 Collaborations J. Ahrens *et al.*, *Phys. Rev. Letts.* **87**, 022003 (2001), hep-ex/0105089.
18. D. Drechsel *et al.*, *Nucl. Phys.* **A645**, 145 (1999).
19. N. Bianchi and T. Thomas, *Phys. Lett.* **B450**, 439 (1999).

20. H. Burkhardt and W. N. Cottingham, *Ann. Phys. (N.Y.)* **56**, 453 (1970).
21. K. Griffioen, Talk presented at this Symposium (2001).
22. J. Soffer and O. V. Teryaev, *Phys. Rev. Lett.* **70**, 3371 (1993).
23. V. Burkert and B. Ioffe, *Phys. Lett.* **B296**, 223 (1992); *J. Exp. Theo. Phys.* **78**, 619 (1994).
24. J. P. Chen, Talk presented at this Symposium (2001).
25. D. Drechsel *et al.*, *Phys. Rev.* **D63**, 114010 (2001).
26. E. D. Bloom and F. J. Gilman, *Phys. Rev. Lett.* **25**, 1140 (1970); *Phys. Rev.* **D4**, 2901 (1971).
27. I. Niculescu *et al.*, *Phys. Rev. Lett.* **85**, 1182, 1186 (2000).
28. T. Gehrmann and W. J. Stirling, *Phys. Rev.* **D53**, 6100 (1996).
29. E. Shuryak and A. Vainshtein, *Nucl. Phys.* **B201**, 141 (1982).
30. R. Jaffe and X. Ji, *Phys. Rev.* **D43**, 724 (1991).
31. J. L. Cortes, B. Pire and J. P. Ralston, *Z. Phys.* **C55**, 409 (1992).
32. S. Wandzura and F. Wilczek, *Phys. Lett.* **B72**, 195 (1977).
33. P. Bosted, Talk presented at this Symposium (2001).
34. Z. Meziani, Talk presented at this Symposium (2001).
35. A. V. Efremov, O. V. Teryaev and E. Leader, *Phys. Rev.* **D55**, 4307 (1997).
36. The SMC Collaboration, B. Adeva *et al.*, *Phys. Lett.* **B369**, 93 (1996).
37. The SMC Collaboration, B. Adeva *et al.*, *Phys. Lett.* **B420**, 180 (1998).
38. The HERMES Collaboration, K. Ackerstaff *et al.*, *Phys. Rev. Lett.* **81**, 5519 (1998).
39. The E866 Collaboration, E. A. Hawker *et al.*, *Phys. Rev. Lett.* **80**, 3715 (1998).
40. The E866 Collaboration, J. C. Peng *et al.*, *Phys. Rev.* **D58**, 092004 (1998).
41. G. T. Garvey and J. C. Peng, *Prog. Part. Nucl. Phys.* **47**, 203 (2001), nucl-ex/0109010.
42. The HERMES Collaboration, K. Ackerstaff *et al.*, *Phys. Lett.* **B464**, 123 (1999).
43. T.-A. Shibata, Talk presented at this Symposium (2001).
44. S. Bernreuther, Talk presented at this Symposium (2001).
45. D. I. Diakonov *et al.*, *Phys. Rev.* **D56**, 4069 (1997).
46. C. Bourrely and J. Soffer, *Phys. Lett.* **B314**, 132 (1993).
47. C. Bourrely and J. Soffer, *Nucl. Phys.* **B423**, 329 (1994).
48. J. Kirluk, Talk presented at this Symposium (2001).
49. N. Saito, Talk presented at this Symposium (2001).
50. The HERMES Collaboration, A. Airapetian *et al.*, *Phys. Rev. Lett.* **84**, 2584 (2000).
51. COMPASS proposal, CERN/SPSLC-96-14 (March, 1996).
52. <http://www.slac.stanford.edu/exp/e161>.
53. M. Liu, Talk presented at this Symposium (2001).
54. J. Collins, *Nucl. Phys.* **B396**, 161 (1993); *Nucl. Phys.* **B420**, 565 (1994).
55. A. V. Efremov, O. G. Smirnova and L. G. Tkachev, *Nucl. Phys. Proc. Suppl.* **74**, 49 (1999).
56. G. Schnell, Talk presented at this Symposium (2001).
57. The HERMES Collaboration, A. Airapetian *et al.*, *Phys. Rev. Lett.* **84**, 4047 (2000).
58. The HERMES Collaboration, A. Airapetian *et al.*, *Phys. Rev.* **D64**, 097101 (2001).
59. K. A. Oganessian, H. R. Avakian, N. Bianchi and A. M. Kotzinian, hep-ph/9808368.
60. E. De Sanctis, W.-D. Nowak and K. A. Oganessian, *Phys. Lett.* **B483**, 69 (2000).
61. A. Bravar for the SMC Collaboration, *Nucl. Phys. Proc. Suppl.* **79**, 520 (1999).
62. V. A. Korotkov, W. -D. Nowak and K. A. Oganessian, *Eur. Phys. J.* **C18**, 639 (2001).
63. X. Ji, *Phys. Rev. Lett.* **78**, 610 (1997); *Phys. Rev.* **D55**, 7114 (1997).
64. The ZEUS Collaboration, P. R. B. Saull, Proceedings of the International Europhysics Conference on High-Energy Physics, Tampere, Finland, 420-422 (1999), hep-ex/0003030.

65. The H1 Collaboration, C. Adloff *et al.*, *Phys. Lett.* **B517**, 47 (2001).
66. The HERMES Collaboration, A. Airapetian *et al.*, *Phys. Rev. Lett.* **87**, 182001 (2001).
67. The CLAS Collaboration, S. Stepanyan *et al.*, *Phys. Rev. Lett.* **87**, 182002 (2001).
68. N. Bianchi, Talk presented at this Symposium (2001).
69. M. Diehl *et al.*, *Phys. Lett.* **B411**, 193 (1997).
70. The ALEPH Collaboration, D. Buskulic *et al.*, *Phys. Lett.* **B374**, 319 (1996).
71. The OPAL Collaboration, K. Ackerstaff *et al.*, *Eur. Phys. J.* **C2**, 49 (1998).
72. The NOMAD Collaboration, P. Astier *et al.*, *Nucl. Phys.* **B588**, 3 (2000).
73. The NOMAD Collaboration, P. Astier *et al.*, *Nucl. Phys.* **B605**, 3 (2001).
74. The E665 Collaboration, M. R. Adams *et al.*, *Eur. Phys. J.* **C17**, 263 (2000).
75. The HERMES Collaboration, A. Airapetian *et al.*, *Phys. Rev.* **D64**, 112005 (2001).
76. D. de Florian, M. Stratmann and W. Vogelsang, *Phys. Rev.* **D57**, 5811 (1998).
77. B. Q. Ma, I. Schmidt and J. J. Yang, *Phys. Lett.* **B477**, 107 (2000).
78. J. C. Collins *et al.*, *Phys. Rev.* **D56**, 2982 (1997).
79. M. Vanderhaeghen *et al.*, *Phys. Rev.* **D60**, 094017 (1999).
80. The HERMES Collaboration, A. Airapetian *et al.*, hep-ex/0112022.
81. The CLAS Collaboration, R. De Vita *et al.*, *Phys. Rev. Lett.* **88**, 082001 (2002).
82. G. R. Farrar and D. R. Jackson, *Phys. Rev. Lett.* **35**, 1416 (1975).
83. S. Brodsky, M. Burkardt and I. Schmidt, *Nucl. Phys.* **B441**, 197 (1995).
84. G. Bunce, Talk presented at this Symposium (2001).